





Article

# A Hexahomotrioxacalix[3]arene-Based Ditopic Receptor for Alkylammonium Ions Controlled by Ag<sup>+</sup> Ions

Xue-Kai Jiang <sup>1</sup>, Yusuke Ikejiri <sup>1</sup>, Chong Wu <sup>1</sup>, Shofiur Rahman <sup>2</sup>, Paris E. Georghiou <sup>2</sup> , Xi Zeng <sup>3</sup>, Mark R. J. Elsegood <sup>4</sup> , Carl Redshaw <sup>5</sup> , Simon J. Teat <sup>6</sup>  and Takehiko Yamato <sup>1,\*</sup>

<sup>1</sup> Department of Applied Chemistry, Faculty of Science and Engineering, Saga University, Honjo-machi 1, Saga 840-8502 Japan; jxk1215@163.com (X.K.J.); k1xshamgod@gmail.com (Y.I.); wuchong214@163.com (C.W.)

<sup>2</sup> Department of Chemistry, Memorial University of Newfoundland, St. John's, NL A1B 3X7, Canada; mdrahman71@yahoo.com (S.R.); parisg@mun.ca (P.E.G.)

<sup>3</sup> Key Laboratory of Macrocyclic and Supramolecular Chemistry of Guizhou Province, Guizhou University, Guiyang 550025, China; zengxi1962@163.com

<sup>4</sup> Chemistry Department, Loughborough University, Loughborough, LE11 3TU, UK; M.R.J.Elsegood@lboro.ac.uk

<sup>5</sup> Chemistry, School of Mathematics and Physical Sciences, The University of Hull, Cottingham Road, Hull, Yorkshire, HU6 7RX, UK; C.Redshaw@hull.ac.uk

<sup>6</sup> ALS, Berkeley Lab, 1 Cyclotron Road, Berkeley, CA 94720, USA; sjteat@lbl.gov

\* Correspondence: yamatot@cc.saga-u.ac.jp; Tel.: +81-952-28-8679; Fax: +81-952-28-8679

Received: 18 December 2017; Accepted: 5 February 2018; Published: 21 February 2018

**Abstract:** A receptor *cone-1* based on a hexahomotrioxacalix[3]arene bearing three pyridyl groups was successfully synthesized, which has a C<sub>3</sub>-symmetric conformation and is capable of binding alkylammonium and metal ions simultaneously in a cooperative fashion. It can bind alkylammonium ions through the π-cavity formed by three aryl rings. This behaviour is consistent with the cone-in/cone-out conformational rearrangement needed to reorganize the cavity for *endo*-complexation. As a C<sub>3</sub>-symmetrical pyridyl-substituted calixarene, receptor *cone-1* can also bind an Ag<sup>+</sup> ion, and the nitrogen atoms are turned towards the inside of the cavity and interact with Ag<sup>+</sup>. After complexation of tris(2-pyridylamide) derivative receptor *cone-1* with Ag<sup>+</sup>, the original C<sub>3</sub>-symmetry was retained and higher complexation selectivity for *n*-BuNH<sub>3</sub><sup>+</sup> versus *t*-BuNH<sub>3</sub><sup>+</sup> was observed. Thus, it is believed that this receptor will have a role to play in the sensing, detection, and recognition of Ag<sup>+</sup> and *n*-BuNH<sub>3</sub><sup>+</sup> ions.

**Keywords:** hexahomotrioxacalix[3]arene; alkylammonium ions; metal ions; ditopic receptor; allosteric effects

## 1. Introduction

Over the past few decades, the development of artificial receptors for ion recognition, complexation, and transportation has proven to be an important topic in both environmental and supramolecular chemistry [1–4]. Given their ready availability, and their unique conformational and cavity-containing structures, together with their versatile molecular recognition properties, calixarenes have attracted a great deal of attention during the past several decades, and, indeed, calixarene chemistry has become an indispensable part of supramolecular science [5–9]. Calix[*n*]arenes can provide useful building blocks for host-guest type receptors by appropriate modification. For example, calix[4]arene derivatives incorporating crown ethers, amides, esters, and carboxylic acid groups have been shown to selectively extract metal ions [10]. Hexahomotrioxacalix[3]arenes, which are structurally related to both calixarenes and to crown ethers, have a three dimensional cavity with a

potentially  $C_3$ -symmetric structure, and have been shown to be useful ligands for metal cations [11–14], ammonium cations [15,16], and fullerene derivatives [17,18].

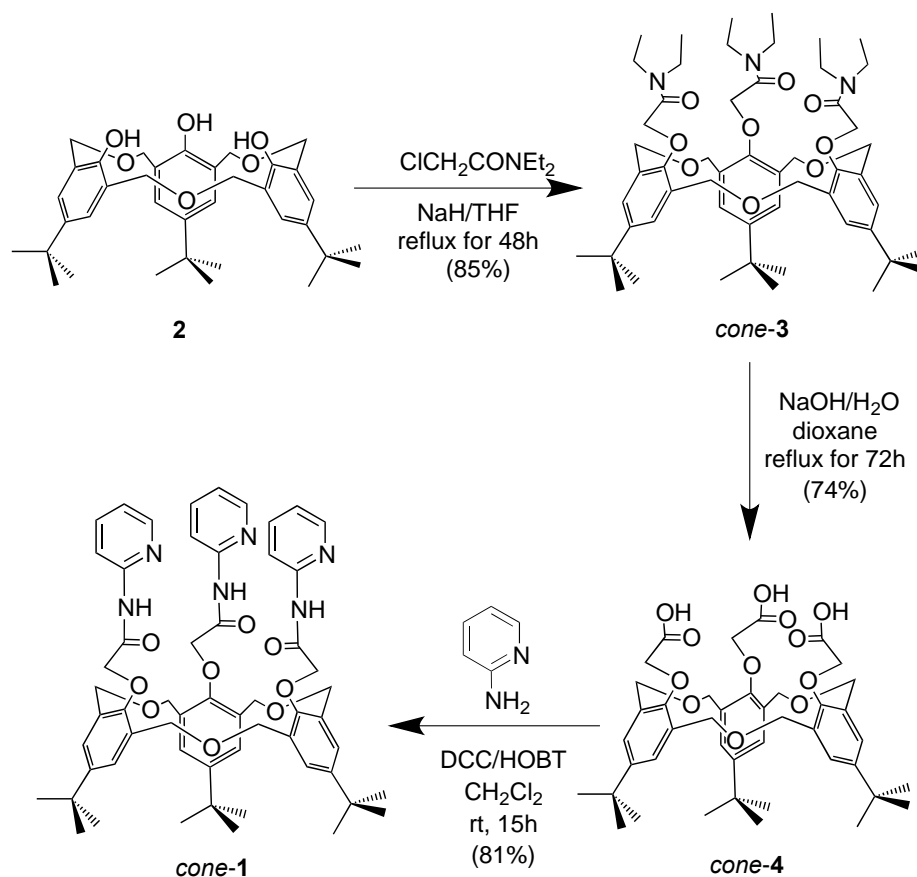
Cation recognition by artificial receptors has attracted increasing attention due to the important roles played by ions in both environmental and biological systems [19,20]. All the known modes of cation binding by native and functionalized calixarenes exploit cation- $\pi$  induced dipoles, or electrostatic interactions [21]. The most important calixarene-based cation receptors are obtained by the introduction of chelating units at the lower rather than at the upper rim. For example, calixarenes fully functionalized at the lower rim with ether groups show an affinity for alkali metal ions [22–25]. Shinkai et al. reported a series of calix[4]arene-crown-4 derivatives, among which a *partial-cone* derivative exhibits an exceptional  $Na^+/K^+$  selectivity, as determined by ion-selective electrodes (ISEs) [23]. We also have developed a series of triazole-derived chemosensors for selective binding of heavy metal ions based on hexahomotrioxacalix[3]arene and thiacalix[4]arene scaffolds [26–28]. For example, chemosensors derived from hexahomotrioxacalix[3]arene appended at the lower rim with pyrenyl groups via triazole linkers exhibited a highly selective affinity for the  $Pb^{2+}$  cation through enhancement of the monomer emission of the pyrene moiety in both organic and organic-aqueous solution [26].

On the other hand, hexahomotrioxacalix[3]arene derivatives that have  $C_3$  symmetry can also selectively bind ammonium ions, which play an important role in both chemistry and biology. The formation of intra-cavity *endo*-complexes of the resulting alkylammonium ions have been reported. Tripodal  $NH^+ \cdots O$  interactions with the phenolic oxygen atoms and  $C-H \cdots \pi$  interactions stabilized the complex [1–4,11]. Recently, our group reported the construction of  $C_3$  symmetrically functionalized hexahomotrioxacalix[3]arenes, which selectively recognized primary alkylammonium ions [29,30].

It is against this background that we describe herein the design, synthesis, and binding properties of receptor *cone-1*, based on hexahomotrioxacalix[3]arene, which recognizes alkylammonium cations and  $Ag^+$  with high association constants.

## 2. Results and Discussion

*Cone-1*, which is based on a hexahomotrioxacalix[3]arene, was synthesized by the method shown in Scheme 1. *Cone-3* was prepared by *O*-alkylation of hexahomotrioxacalix[3]arene **2** with *N,N*-diethylchloroacetamide in the presence of NaH in refluxing THF according to the reported procedure in 85% yield [31,32]. *Cone-4* was synthesized in 74% yield by hydrolyzing *cone-3* in a refluxing mixture of NaOH/ $H_2O$ /dioxane solution. The *cone*-hexahomotrioxacalix[3]arene triamide derivative (*cone-1*) was prepared in 81% yield by a condensation reaction between *cone-4* and 2-aminopyridine in the presence of DCC (dicyclohexylcarbodiimide) and HOBt (1-hydroxybenzotriazole) at room temperature for 15 h in  $CH_2Cl_2$ .



**Scheme 1.** Synthesis of receptor *cone-1*.

In agreement with its  $C_3$ -symmetric *cone-in* conformation, receptor *cone-1* displays the following characteristic  $^1\text{H}$  and  $^{13}\text{C}$ -NMR spectroscopic features: (1) the *cone-1* conformation is firmly established by the presence of the bridging methylene protons that have a  $\Delta\delta$  separation between  $\text{H}_{\text{ax}}$  and  $\text{H}_{\text{eq}}$  of  $\Delta\delta$  0.41 ppm in the  $^1\text{H}$ -NMR spectrum ( $\text{CDCl}_3$ ). In the calix[4]arenes, the  $\Delta\delta$  values of the  $\text{ArCH}_2\text{Ar}$  methylene protons have been correlated with the orientation of the adjacent aromatic rings [33,34] and similar findings were previously observed with hexahomotrioxacalix[3]arenes [12,13]. (2) The  $^{13}\text{C}$ -NMR spectrum of receptor *cone-1* in  $\text{CDCl}_3$  exhibited two peaks at  $\delta$  31 and 34 ppm for the *tert*-butyl carbons and a single peak at  $\delta$  69 ppm for the  $-\text{OCH}_2-$  bridge linker carbons [35]. (3) The  $^1\text{H}$ -NMR spectrum of receptor *cone-1* in  $\text{CDCl}_3$  revealed a single peak at  $\delta$  1.15 ppm for the *tert*-butyl protons and a single peak at  $\delta$  6.99 ppm for the aromatic protons, which was in agreement with a  $C_{3v}$ -symmetric structure [36].

Single crystal X-ray diffraction studies of *cone-1* shows a rather deformed *cone* conformation (Figure 1). *Cone-1* crystallises as solvates incorporating either three methanol molecules, and one water molecule or with  $2\frac{1}{2}$  methanol molecules. Within each calixarene is a single  $\text{N-H}\cdots\text{O}$  H-bond between a secondary amine moiety and a single ether oxygen atom. See experimental section and Table S1 for crystal data.

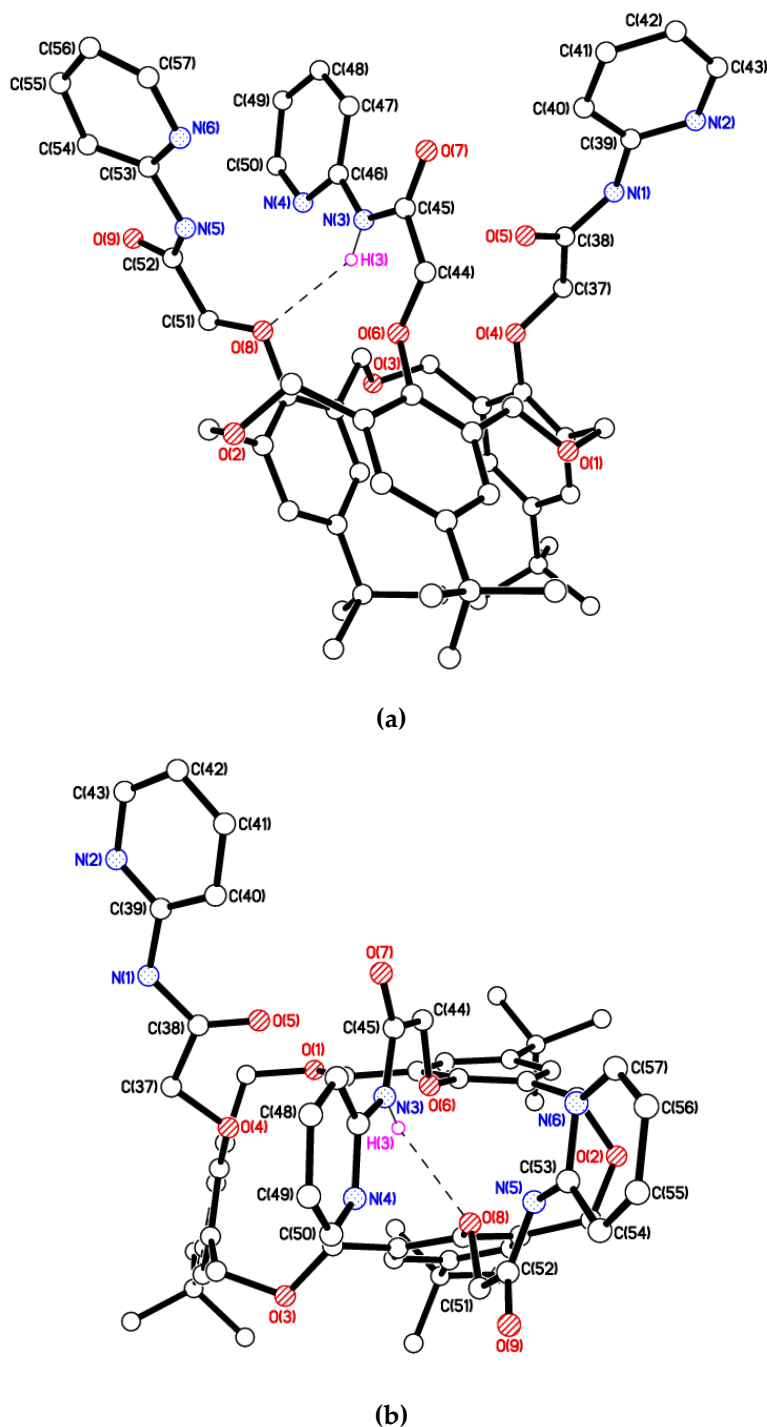


**Figure 1.** Side-view (a) and top-view (b) of the X-ray structure of *cone-1*. H-bonds shown as dashed lines;  $H(3)\cdots O(8) = 2.29(2) \text{ \AA}$ ,  $\angle N(3)-H(3)\cdots O(8) = 147(2)$ . Solvent molecules of crystallization and H atoms not involved in H-bonding omitted for clarity.

In *cone-1*·3 MeOH·H<sub>2</sub>O the calixarene molecule adopts a collapsed, or squashed, conformation to facilitate this H-bond and a  $\pi\cdots\pi$  interaction between the arene rings C(13)–C(18) and C(25)–C(30), at a distance of 3.87 Å. The pyridyl groups C(46)–N(4) and C(53)–N(6) are aligned face-to-face but at a distance of 4.80 Å, which is too far for  $\pi\cdots\pi$  stacking to be adopted. The structure of *cone-1*·2.5 MeOH is very similar and is isomorphous (see Figures S7 and S8).

In order to investigate the ionophoric affinities of the receptor *cone-1* for alkylammonium ions, the binding properties of receptor *cone-1* as a ditopic receptor were investigated by means of  $^1\text{H-NMR}$  spectroscopic titration experiments, using *n*-butylammonium and *t*-butylammonium picrates as the substrates. Binding studies were carried out by adding increasing amounts of the appropriate salt to a 5.0 mM solution of receptor *cone-1* in  $\text{CDCl}_3/\text{CD}_3\text{CN}$  co-solvent, so as to reach a 1:1 host/guest ratio. In the case of  $n\text{-BuNH}_3^+$ , the proton signals of receptor *cone-1* were observed for both the complex and the free host, as shown in Figure 2. Upon increasing the amount of alkylammonium ions, the signals for receptor *cone-1* decreased, and, finally, only signals for the complex were observed. Host-guest complexation/decomplexation was judged to be slow on the NMR time scale on the basis of preliminary titration experiments, which, in the presence of greater host than guest concentrations, revealed broadness for the receptor *cone-1* peaks. The peak assigned to the aromatic hydrogen atoms of the hexahomotrioxacalix[3]arene unit underwent a significant down-field complexation-induced shift (CIS) (from  $\delta$  6.99 to 7.31 ppm), indicating that the cavity was ‘opening-up’ to make room for the incoming cationic guest.

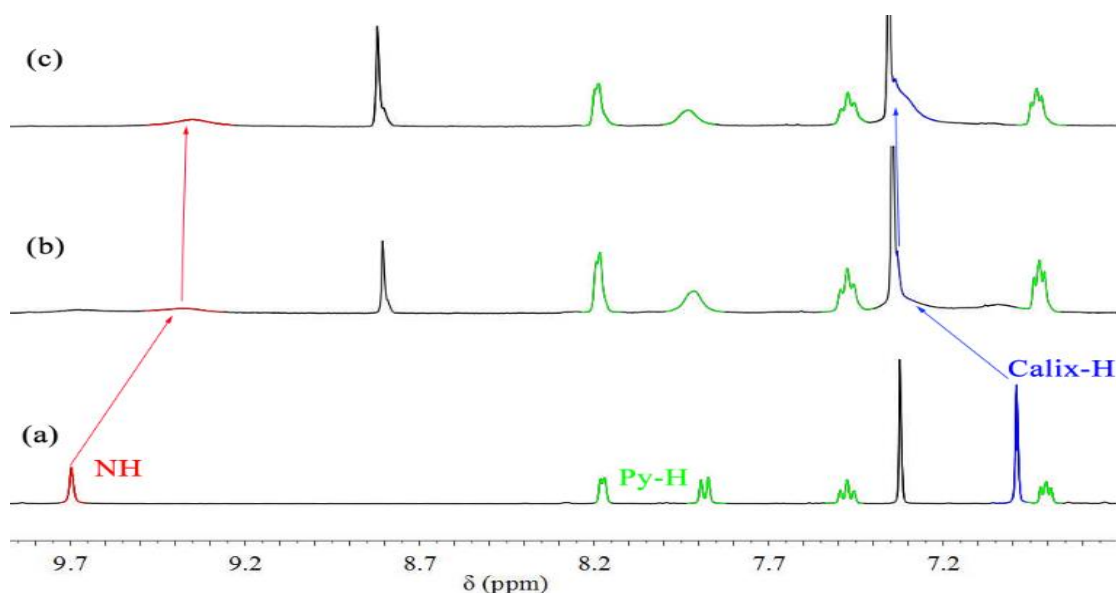


**Figure 2.** Partial  $^1\text{H-NMR}$  spectra of receptor *cone-1* (5.0 mM) in  $\text{CDCl}_3/\text{CD}_3\text{CN}$  (10:1, *v/v*); (a) *cone-1*; (b) *cone-1*  $\supset$   $n\text{-BuNH}_3^+$  (0.6 equiv.); (c) *cone-1*  $\supset$   $n\text{-BuNH}_3^+$  (1.0 equiv.).

This behaviour is consistent with a *cone-in-cone-out* conformational rearrangement needed to reorganize the cavity upon *endo*-complexation. On the other hand, there are two modes for receptor *cone-1* to bind with *n*-butylammonium ions, i.e., either at the lower rim through the substituent moieties, or at the upper rim through the  $\pi$ -cavity formed by the three aromatic rings (Figure 3). The presence of the target  $n\text{-BuNH}_3^+$  cation was evident from the appearance of high-field resonances for the included *n*-butyl chain as presented in Table 1 [37,38]. It suggests that the alkyl protons of the  $n\text{-BuNH}_3^+$  ion reside inside the cavity of receptor *cone-1* and are subjected to a shielding effect from the phenyl rings (Figure 3a) [39–42]. This evidence suggests the binding occurs through the  $\pi$ -cavity formed by the three aromatic rings of the hexahomotrioxacalix[3]arene unit. This binding is attributed to the  $\pi$ -effect of the aromatic rings and is favoured, since both the host and the guest molecules have  $\text{C}_3$ -symmetric conformations.

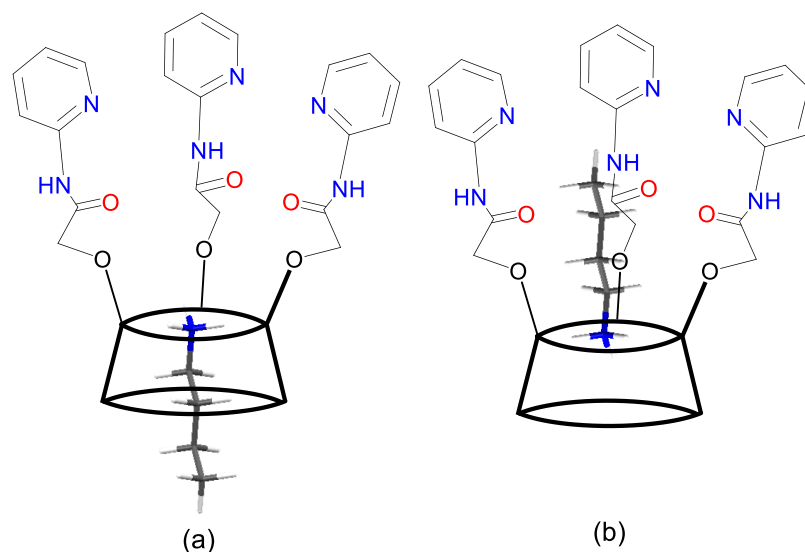


**Figure 3.** Two possible interactions between receptor *cone-1* and  $n\text{-BuNH}_3^+$ .

**Table 1.** Selected proton chemical shifts ( $\delta$ , ppm) (300 MHz,  $\text{CDCl}_3:\text{CD}_3\text{CN}$ , 10:1  $v/v$ , 27 °C) of guest. <sup>a</sup>

|                     |                | Chemical Shift of Proton |                          |                                     |               |
|---------------------|----------------|--------------------------|--------------------------|-------------------------------------|---------------|
|                     |                | $\text{CH}_3$            | $\text{CH}_3\text{CH}_2$ | $\text{CH}_3\text{CH}_2\text{CH}_2$ | $\text{CH}_2$ |
| $n\text{-BuNH}_3^+$ | Free           | 0.94                     | 1.40                     | 1.67                                | 3.02          |
|                     | Complex        | 0.88                     | 0.30                     | -0.33                               | 0.30          |
|                     | $\Delta\delta$ | -0.06                    | -1.10                    | -2.00                               | -2.72         |
| $t\text{-BuNH}_3^+$ | Free           | 1.40                     |                          |                                     |               |
|                     | Complex        | -0.34                    |                          |                                     |               |
|                     | $\Delta\delta$ | -1.74                    |                          |                                     |               |

<sup>a</sup> chemical shift ( $\delta$ ): ppm.  $\Delta\delta = \delta_{\text{complex}} - \delta_{\text{free}}$ .

Similar  $^1\text{H-NMR}$  spectroscopic titration experiments were conducted to assess the effect of  $t\text{-BuNH}_3^+$ , and the spectral changes upon complexation are shown in Table 1 and Figure S3. The association constants of receptor *cone-1* with alkylammonium ions were determined and are presented in Table 2. It can be seen that the association constants were affected by the sizes of the respective alkyl groups. Thus, receptor *cone-1* binds more readily to the linear alkyl chain ammonium ion than to the branched chain ammonium ion. These findings might be attributable to the greater ease of entering the cavity for the linear alkyl chain analogs, as well as the slower decomplexation rate of the ammonium ions.

**Table 2.** Association constants  $K_a$  ( $\text{M}^{-1}$ ) of host receptor *cone-1* with alkylammonium ions, with and without  $\text{Ag}^+$  picrate salt. <sup>a,b</sup>

|   | $K_a$ ( $\text{M}^{-1}$ ) |
|---|---------------------------|
| $n\text{-BuNH}_3^+$   | $2680 \pm 155$            |
| $n\text{-BuNH}_3^+ \subset [\text{cone-1} \supset \text{Ag}^+]$ | $3270 \pm 190$            |
| $t\text{-BuNH}_3^+$   | $360 \pm 20$              |
| $t\text{-BuNH}_3^+ \subset [\text{cone-1} \supset \text{Ag}^+]$ | No complexation           |

<sup>a</sup> Measured in  $\text{CDCl}_3/\text{CD}_3\text{CN}$  (10:1,  $v/v$ ) at 27 °C by the  $^1\text{H-NMR}$  titration method, noting the chemical shift change of the NH proton; host concentration was 5.0 mM. <sup>b</sup> Alkylammonium cations were used as their picrate salts.

On the other hand, host receptor *cone-1* was recently reported by us to also have excellent affinity and high selectivity for  $\text{Ag}^+$ ,  $\text{Cu}^{2+}$ , and  $\text{Al}^{3+}$  ions during extraction studies [31,42]. In particular, we reported that receptor *cone-1* exhibited higher extractability for  $\text{Ag}^+$  (76.9%), with the  $\text{Ag}^+$  being

complexed by the three pyridine groups via N–Ag<sup>+</sup> interactions. Therefore, in order to determine optimized conditions for recognition and selectivity of the ammonium ions, the effects on <sup>1</sup>H-NMR spectroscopic titrations of *cone-1*·Ag<sup>+</sup> toward ammonium ions were studied in CDCl<sub>3</sub>/CD<sub>3</sub>CN (10:1, *v/v*). In the case of *n*-BuNH<sub>3</sub><sup>+</sup>, partial <sup>1</sup>H-NMR spectra (Figure 4) revealed that the proton resonances of the *n*-butyl chain were shifted upfield and the proton resonances of the aromatic hydrogen atoms of the hexahomotrioxacalix[3]arene units were shifted downfield by 0.11 ppm (from 6.99 to 7.29 ppm). These findings imply that Ag<sup>+</sup> was encapsulated into the cavity formed by the pyridine rings, and the receptor *cone-1* ‘stands up’ when *n*-BuNH<sub>3</sub><sup>+</sup> is included, because *n*-BuNH<sub>3</sub><sup>+</sup> enters into the cavity formed by the three aromatic rings.

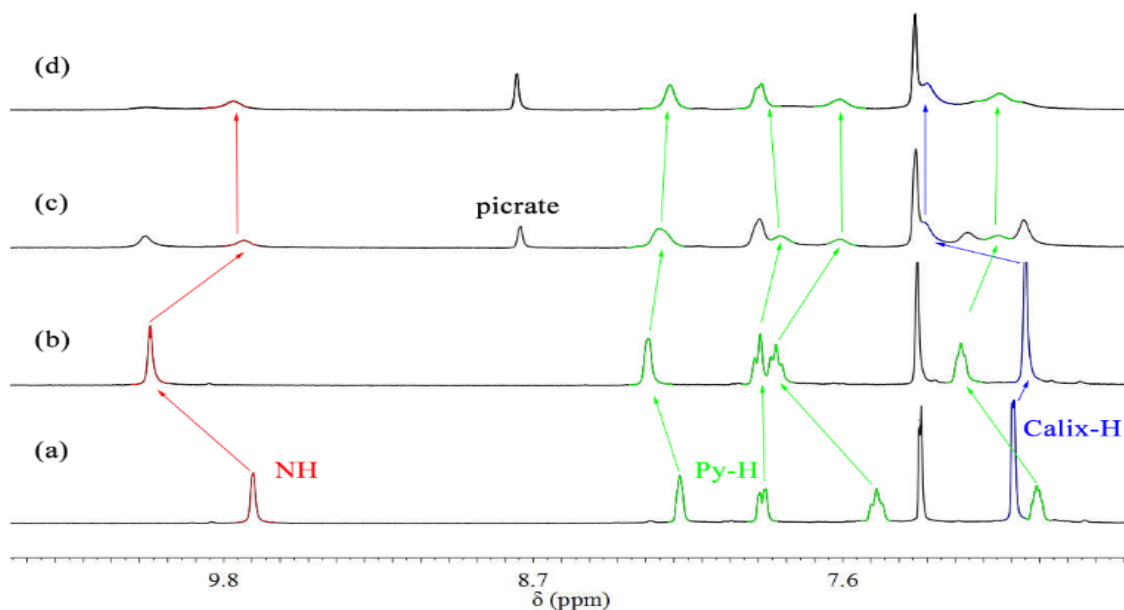


**Figure 4.** Partial <sup>1</sup>H-NMR spectra of receptor *cone-1* (CDCl<sub>3</sub>/CD<sub>3</sub>CN (10:1, *v/v*), 5.0 mM); (a) *cone-1*; (b) *cone-1* ⊃ Ag<sup>+</sup> (1.0 equiv.); (c) *cone-1* ⊃ Ag<sup>+</sup> (1.0 equiv.) ⊃ *n*-BuNH<sub>3</sub><sup>+</sup> (0.5 equiv.); (d) *cone-1* ⊃ Ag<sup>+</sup> (1.0 equiv.) ⊃ *n*-BuNH<sub>3</sub><sup>+</sup> (1.0 equiv.).

Receptor *cone-1* is capable of binding both Ag<sup>+</sup> and *n*-BuNH<sub>3</sub><sup>+</sup> simultaneously in a cooperative fashion. Thus, the potential to act as a ditopic receptor to complex with these two cations will be of great interest in coordination chemistry. Interestingly, similar <sup>1</sup>H-NMR spectroscopic titration experiments were conducted to assess the effect of *t*-BuNH<sub>3</sub><sup>+</sup>, but no significant changes in the resulting <sup>1</sup>H-NMR spectra were observed. Thus, it is evident that receptor *cone-1* has lost the capacity to bind *t*-BuNH<sub>3</sub><sup>+</sup> when in the presence of Ag<sup>+</sup> ion.

When the order of addition of Ag<sup>+</sup> and alkylammonium ions was changed, in the case of *n*-BuNH<sub>3</sub><sup>+</sup>, the resulting <sup>1</sup>H-NMR spectrum is identical to that obtained in the previous section (Figure S4). Furthermore, in the case of *t*-BuNH<sub>3</sub><sup>+</sup>, the resulting final <sup>1</sup>H-NMR spectrum is the same as that for the complex *cone-1*·Ag<sup>+</sup>. These findings indicate that receptor *cone-1* does not selectively recognize alkylammonium ions efficiently in the absence of Ag<sup>+</sup> ion. Interestingly, when Ag<sup>+</sup> ion was added to the present system, Ag<sup>+</sup> provided an excellent pathway of organizing alkylammonium ions binding groups for optimal host-guest interactions by adjusting the size of the cavity of receptor *cone-1*. The association constants of receptor *cone-1* with the alkylammonium ions in the absence of and in the presence of Ag<sup>+</sup> as calculated from the chemical shift changes of the NH protons are summarized in Table 2. Interestingly, the association constant *K*<sub>a</sub> for the complexation of receptor *cone-1* with *n*-BuNH<sub>3</sub><sup>+</sup> (*K*<sub>a</sub> = 2680 ± 155) is much larger than that when using *t*-BuNH<sub>3</sub><sup>+</sup> (*K*<sub>a</sub> = 360 ± 20). Thus, in the presence of Ag<sup>+</sup>, the complexation with *n*-BuNH<sub>3</sub><sup>+</sup> increases compared with *t*-BuNH<sub>3</sub><sup>+</sup>, presumably due to the different cavity size of receptor *cone-1*.

The geometries of the molecular structures were optimized with the PBE0 functional theory with the LANL2DZ basis set. The DFT level of theory used the hybrid Perdew-Burke-Ernzerhof parameter free-exchange correlation functional PBE0 (PBE1PBE in the Gaussian realization) [43,44] with the Hay and Wadt effective core potential LANL2DZ basis set [45–47]. The starting structure was generated using SpartanPro10 with the MMFF94 method [48]. The generated structures were then imported into Gaussian-09 Revision D.01 (Wallingford, CT, USA) [49], and were geometry-optimized in the gas phase. The calculated binding or interaction energies (IE) for *cone-1* ⊃ *n*-BuNH<sub>3</sub><sup>+</sup>, *cone-1* ⊃ *t*-BuNH<sub>3</sub><sup>+</sup>, *cone-1* ⊃ Ag<sup>+</sup>, and *n*-BuNH<sub>3</sub><sup>+</sup> ⊃ [*cone-1* ⊃ Ag<sup>+</sup>] are −298.8 kJ mol<sup>−1</sup>; −268.3 kJ·mol<sup>−1</sup>; −457.1 kJ·mol<sup>−1</sup>, and −525.8 kJ·mol<sup>−1</sup>, respectively, and were in agreement with the trend for the observed complexation data obtained by the <sup>1</sup>H-NMR spectroscopic titration experiments (Figure 5). A conceptualization of complexation by the receptor *cone-1* is shown in Figure 6.

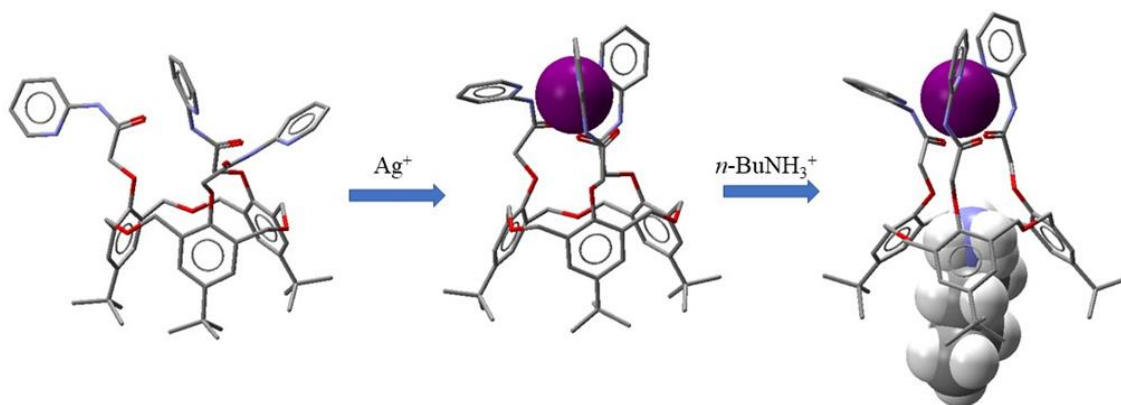


**Figure 5.** Geometry-optimized (PBE0/LANL2DZ) structures of *cone-1* and its complex with Ag<sup>+</sup> and *n*-BuNH<sub>3</sub><sup>+</sup>. Left: The free *cone-1*, Middle: 1:1 *cone-1* ⊃ Ag<sup>+</sup> complex, and Right: *n*-BuNH<sub>3</sub><sup>+</sup> ⊃ [*cone-1* ⊃ Ag<sup>+</sup>] complex. Colour code: carbon = black grey, oxygen atom = red, nitrogen = blue, nitrogen (*n*-BuNH<sub>3</sub><sup>+</sup>) = magenta and Ag<sup>+</sup> = purple. Hydrogen atoms on the host molecule have been removed for clarity.

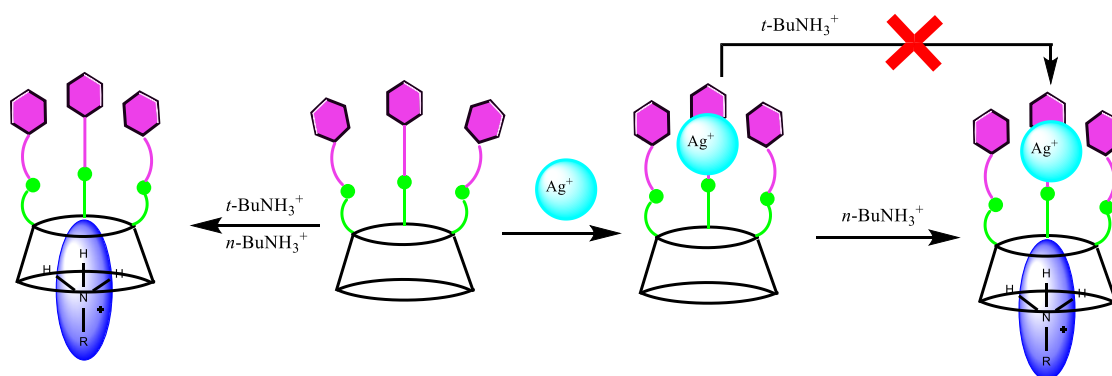


**Figure 6.** A plausible binding model. The green circles represent the -CONH-, and the hexagons (purple color) represent the pyridyl groups.

### 3. Experimental Section

#### 3.1. General

All melting points were determined using a Yanagimoto MP-S1 melting point apparatus (Kyoto, Japan). <sup>1</sup>H-NMR spectra were recorded at 300 MHz with a Nippon Denshi JEOL FT-300 NMR spectrometer (Tokyo, Japan) with SiMe<sub>4</sub> as an internal reference; *J* values are given in Hz. IR spectra were measured as KBr pellets on a Nippon Denshi JIR-AQ20M spectrophotometer. UV-vis. spectra



were measured with a Shimadzu 240 spectrophotometer (Tokyo, Japan). Mass spectra were obtained on a Nippon Denshi JMS-01SG-2 mass spectrometer at an ionization energy of 70 eV using a direct inlet system through GLC. Elemental analyses were performed with a Yanaco MT-5 (Kyoto, Japan).

### 3.2. Materials

Synthesis of *cone-7,15,23-tri-tert-butyl-25,26,27-tris[(N,N-diethylaminocarbonyl)methoxy]-2,3,10,11,18,19-hexahomo-3,11,19-trioxacalix[3]arene (cone-3)* was carried out according to the previously reported procedure [31].

### 3.3. Preparation of *cone-4*

A mixture of *cone-3* (500 mg, 0.55 mmol) and 15 mL of an aqueous 1.0 M NaOH solution in dioxane (15 mL) was heated at reflux for 72 h under N<sub>2</sub>. After cooling the reaction mixture to room temperature, the solution was acidified with 1 M HCl (pH 1–2) and extracted three times (30 mL × 3) with ethyl acetate. The organic layer was separated, dried (MgSO<sub>4</sub>), and the solvent was evaporated. The residue was dried to afford *cone-4*, which was washed with methanol to afford the desired product *cone-4* as a white solid (320 mg, 74%), m.p. 227–229 °C (lit. [42], m.p. 227–229 °C).

### 3.4. Preparation of *cone-1*

A solution of *cone-4* (100 mg, 0.13 mmol), 2-aminopyridine (120 mg, 1.11 mmol), and HOBt (75 mg, 0.49 mmol) in dry CH<sub>2</sub>Cl<sub>2</sub> (15 mL) was cooled in an ice bath. DCC (560 mg, 2.71 mmol) and dry CH<sub>2</sub>Cl<sub>2</sub> (5 mL) were added, and the mixture was stirred for an additional 15 h at r.t., and then the solvent was evaporated. The residue was extracted three times (3 × 30 mL) with ethyl acetate. The organic layer was separated, dried (MgSO<sub>4</sub>), and the solvent was evaporated. The residue was dried to afford **1** as a colourless oil, which was recrystallized from CHCl<sub>3</sub>–hexane (1:3 *v/v*) to afford the desired product *cone-1* (85 mg, 81%) as colourless prisms. M.p. 217–218 °C. IR:  $\nu_{\max}$  (KBr)/cm<sup>-1</sup> 3345, 3015, 2915, 2867, 1758, 1483, 1456, 1363, 1234, 1199, 1094 and 1058. <sup>1</sup>H-NMR (300 MHz, CDCl<sub>3</sub>):  $\delta_{\text{H}}$  = 1.15 (s, 27H, *t*-Bu-H), 4.49 (s, 6H, –CH<sub>2</sub>), 4.53 (d, *J* = 11 Hz, 6H, –OCH<sub>2</sub>), 4.94 (d, *J* = 11 Hz, 6H, –OCH<sub>2</sub>), 6.89 (m, 3H, Py-H), 6.99 (s, 6H, Calix-H), 7.47 (m, 3H, Py-H), 7.87 (d, 3H, *J* = 8.0 Hz, Py-H), 8.17 (d, *J* = 8.0 Hz, 3H, Py-H) and 9.69 (s, 3H, NH) ppm. <sup>13</sup>C-NMR (100 MHz, CDCl<sub>3</sub>):  $\delta_{\text{C}}$  = 31.42, 34.26, 69.65, 73.16, 113.92, 119.65, 126.94, 130.54, 137.58, 147.05, 147.74, 150.74, 152.58 and 167.45 ppm. FABMS: *m/z* calcd for C<sub>57</sub>H<sub>66</sub>N<sub>6</sub>O<sub>9</sub> 978.17 [M<sup>+</sup>]; found 978.45 [M<sup>+</sup>]. C<sub>57</sub>H<sub>66</sub>N<sub>6</sub>O<sub>9</sub> (978.17): calcd C 69.92, H 6.79; found: C 69.74, H 6.93.

### 3.5. <sup>1</sup>H-NMR Spectroscopic Complexation Experiments

To a CDCl<sub>3</sub>/CD<sub>3</sub>CN solution (10:1, *v/v*) of *cone-1* (4 × 10<sup>-3</sup> M) in an NMR tube was added 1.0 equivalent of related metal perchlorates. The spectrum was recorded after addition, and the temperature of the NMR probe was kept constant at 27 °C.

The <sup>1</sup>H-NMR spectroscopic data of the host molecules of the respective complexes only are given below: The <sup>1</sup>H-NMR data of the most representative complexes is given below:

**Receptor *cone-1* ⊃ *n*-BuNH<sub>3</sub><sup>+</sup>**:  $\delta_{\text{H}}$  (CDCl<sub>3</sub>/CD<sub>3</sub>CN, 10:1): 1.24 (s, 27H, *t*-Bu-H), 4.36 (bs, 6H, –OCH<sub>2</sub>), 4.94 (bs, 6H, –CH<sub>2</sub>), 5.32 (bs, 6H, –OCH<sub>2</sub>), 6.91 (m, 3H, Py-H), 7.31 (s, 6H, Calix-H), 7.45 (m, 3H, Py-H), 7.91 (m, 3H, Py-H), 8.17 (d, 3H, *J* = 3.0 Hz, Py-H) and 9.35 (s, 3H, NH) ppm.

**Receptor *cone-1* ⊃ *t*-BuNH<sub>3</sub><sup>+</sup>**:  $\delta_{\text{H}}$  (CDCl<sub>3</sub>/CD<sub>3</sub>CN, 10:1): 1.23 (s, 27H, *t*-Bu-H), 4.49 (bs, 6H, –OCH<sub>2</sub>), 5.11 (bs, 6H, –CH<sub>2</sub>), 5.40 (m, 6H, –OCH<sub>2</sub>), 6.93 (t, *J* = 6.6 Hz, 3H, Py-H), 7.29 (s, 6H, Calix-H), 7.48 (m, 3H, Py-H), 7.91 (m, 3H, Py-H), 8.17 (d, 3H, *J* = 3.0 Hz, Py-H) and 9.35 (s, 3H, NH) ppm.

**Receptor *cone-1* ⊃ Ag<sup>+</sup>**:  $\delta_{\text{H}}$  (CDCl<sub>3</sub>/CD<sub>3</sub>CN, 10:1): 1.01 (s, 27H, *t*-Bu-H), 4.20 (d, *J* = 12.0 Hz, 6H, –OCH<sub>2</sub>), 4.28 (s, 6H, –CH<sub>2</sub>), 4.84 (d, 6H, *J* = 12.0 Hz, –OCH<sub>2</sub>), 6.81 (s, 6H, Calix-H), 7.07 (m, 3H, Py-H), 7.76 (m, 6H, Py-H), 8.17 (d, 3H, *J* = 3.8 Hz, Py-H) and 9.96 (s, 3H, NH) ppm.

**Receptor *cone-1* ⊃ Ag<sup>+</sup> ⊃ *n*-BuNH<sub>3</sub><sup>+</sup>**:  $\delta_{\text{H}}$  (CDCl<sub>3</sub>/CD<sub>3</sub>CN, 10:1): 1.26 (s, 27H, *t*-Bu-H), 4.35 (d, 6H, *J* = 9 Hz, –OCH<sub>2</sub>), 4.99 (d, *J* = 9 Hz, 6H, –CH<sub>2</sub>), 5.32 (b, 6H, –OCH<sub>2</sub>), 7.05 (b, 3H, Py-H), 7.29 (s, 6H,

Calix-H), 7.62 (m, 3H, Py-H), 7.92 (d, 3H,  $J = 7.5$  Py-H), 8.19 (d, 3H,  $J = 4.5$  Hz, Py-H) and 9.80 (s, 3H, NH) ppm.

### 3.6. Single-Crystal X-Ray Diffraction Measurements for cone-1

A suitable single crystal (size *ca.*  $0.30 \times 0.17 \times 0.03$  mm<sup>3</sup>) was selected and mounted on a Bruker APEX 2 CCD diffractometer (Billerica, MA, USA) equipped with synchrotron radiation ( $\lambda = 0.7805$  Å) at ALS Station 11.3.1 [49]. Data were corrected for Lorentz and polarisation effects and for absorption [50]. Crystal data for cone-1·3(CH<sub>4</sub>O)·H<sub>2</sub>O: C<sub>57</sub>H<sub>66</sub>N<sub>6</sub>O<sub>9</sub>·3(CH<sub>4</sub>O)·H<sub>2</sub>O,  $M = 1093.30$ , monoclinic,  $C2/c$ ,  $a = 26.1641(11)$ ,  $b = 15.4995(6)$ ,  $c = 28.5153(11)$  Å,  $\beta = 94.063(3)^\circ$ ,  $V = 11,534.8(8)$  Å<sup>3</sup>,  $Z = 8$ ,  $\mu = 0.09$  mm<sup>-1</sup>, 11,3193 reflections measured, 22,109 unique,  $R_{\text{int}} = 0.074$ ,  $R1[F^2 > 2\sigma(F^2)] = 0.067$ ,  $wR2$  (all data) = 0.205 [51]. The *o*-pyridyl group C(53) > N(6) and the *tert*-butyl group C(7) > C(10) were modelled as fully disordered over two sets of positions. The solvent molecules of crystallisation were modelled using the Platon Squeeze procedure due to substantial disorder [52]. Crystal data for cone-1·2.5(CH<sub>4</sub>O): C<sub>57</sub>H<sub>66</sub>N<sub>6</sub>O<sub>9</sub>·2.5(CH<sub>4</sub>O),  $M = 1059.26$ , monoclinic,  $C2/c$ ,  $a = 26.308(2)$ ,  $b = 15.6159(14)$ ,  $c = 28.644(3)$  Å,  $\beta = 94.1811(15)^\circ$ ,  $V = 11,736.3(18)$  Å<sup>3</sup>,  $Z = 8$ ,  $\mu = 0.08$  mm<sup>-1</sup>, 67,896 reflections measured, 17,827 unique,  $R_{\text{int}} = 0.053$ ,  $R1[F^2 > 2\sigma(F^2)] = 0.059$ ,  $wR2$  (all data) = 0.178 [50]. The *o*-pyridyl group C(51) > N(6) and the *tert*-butyl group C(27) > C(29) were modelled as fully disordered over two sets of positions. The solvent molecules of crystallisation were modelled using the Platon Squeeze procedure due to substantial disorder except for atom O(10) due to its proximity to the disordered ring [52]. Further details of the crystal parameters, data collection conditions, and refinement parameters are summarized in Table S2. CCDC 1500977 & 1817851 contain the supplementary crystallographic data for this paper. These data can be obtained free of charge from The Cambridge Crystallographic Data Centre via [www.ccdc.cam.ac.uk/data\\_request/cif](http://www.ccdc.cam.ac.uk/data_request/cif).

## 4. Conclusions

In conclusion, a novel receptor cone-1 based on hexahomotrioxacalix[3]arene was successfully synthesized, and was found to possess a C<sub>3</sub>-symmetric conformation. It can bind alkylammonium ions through the  $\pi$ -cavity formed by three aryl rings. As a C<sub>3</sub>-symmetrical pyridyl-substituted calixarene, ionophore receptor cone-1 can bind an Ag<sup>+</sup> ion, and after complexation of the tris(2-pyridylamide) derivative receptor cone-1 with Ag<sup>+</sup>, the original C<sub>3</sub>-symmetry has been retained, and the complex showed high selectivity for *n*-BuNH<sub>3</sub><sup>+</sup>, but not for *t*-BuNH<sub>3</sub><sup>+</sup>. Thus, it is believed that this receptor will have a role to play in the sensing, detection, and recognition of Ag<sup>+</sup> and *n*-BuNH<sub>3</sub><sup>+</sup> ions simultaneously.

**Supplementary Materials:** The following are available online, Figure S1: <sup>1</sup>H-NMR spectrum of the synthesized receptor cone-1, Figure S2: <sup>13</sup>C-NMR spectrum of the synthesized receptor cone-1, Figure S3: <sup>1</sup>H-NMR titration experiments for cone-1 with *t*-BuNH<sub>3</sub><sup>+</sup> and Ag<sup>+</sup>, Figure S4: <sup>1</sup>H-NMR titration experiments for cone-1 with *n*-BuNH<sub>3</sub><sup>+</sup> and Ag<sup>+</sup>, Figure S5: molar ratio of Ag<sup>+</sup> with host receptor cone-1, Figure S6:  $K_a$  (association constants) for cone-1·Ag<sup>+</sup>, Table S1: summary of crystal data for cone-1·3MeOH·H<sub>2</sub>O and cone-1·2.5MeOH, Figure S7: Crystal structure of cone-1·2.5MeOH, side view, Figure S8: Crystal structure of cone-1·2.5MeOH, top view Figure S9: top view ball-and-stick cone-1 ⊃ *n*-BuNH<sub>3</sub><sup>+</sup> complex, Figure S10: ball-and-stick cone-1 ⊃ *n*-BuNH<sub>3</sub><sup>+</sup> complex, Figure S11: top view ball-and-stick cone-1 ⊃ *t*-BuNH<sub>3</sub><sup>+</sup> complex, Figure S12: ball-and-stick cone-1 ⊃ *t*-BuNH<sub>3</sub><sup>+</sup> complex, Table S2: calculated distances for selected parameters for the backbones of the host cone-1 and complexes with Ag<sup>+</sup> and *n*-BuNH<sub>3</sub><sup>+</sup> ions (Distance in Å).

**Acknowledgments:** This work was performed under the Cooperative Research Program of the “Network Joint Research Center for Materials and Devices (Institute for Materials Chemistry and Engineering, Kyushu University)”. We thank the OTEC at Saga University and the International Cooperation Projects of Guizhou Province (No. 20137002). The EPSRC is thanked for an overseas travel grant to C.R., and The Advanced Light Source is supported by the Director, Office of Science, Office of Basic Energy Sciences, of the U.S. Department of Energy under Contract No. DE-AC02-05CH11231. The computational work has been assisted by the use of computing resources provided by WestGrid and Compute/Calcul Canada. We thank Dr. Grigory Shamov, Westgrid/U. Manitoba for support.

**Author Contributions:** Xue-Kai Jiang, Yusuke Ikejiri, Wu Chong, and Xi Zeng prepared the cone-1 and performed the <sup>1</sup>H-NMR spectroscopic complexation experiment; Shofiur Rahman and Paris E. Georghiou performed the

computational studies and edited the revisions; Mark R. J. Elsegood, and Simon J. Teat analyzed the X-ray data; Takehiko Yamato and Carl Redshaw wrote the paper.

**Conflicts of Interest:** The authors declare no conflict of interest.

## References

- Schmidtchen, F.P.; Berger, M. Artificial Organic Host Molecules for Anions. *Chem. Rev.* **1997**, *97*, 1609–1646. [[CrossRef](#)] [[PubMed](#)]
- Ikeda, A.; Shinkai, S. Novel Cavity Design Using Calix[*n*]arene Skeletons: Toward Molecular Recognition and Metal Binding. *Chem. Rev.* **1997**, *97*, 1713–1734. [[CrossRef](#)] [[PubMed](#)]
- Morohashi, N.; Narumi, F.; Iki, N.; Hattori, T.; Miyano, S. Thiocalixarenes. *Chem. Rev.* **2006**, *106*, 5291–5316. [[CrossRef](#)] [[PubMed](#)]
- Kim, J.S.; Quang, D.T. Calixarene-Derived Fluorescent Probes. *Chem. Rev.* **2007**, *107*, 3780–3799. [[CrossRef](#)] [[PubMed](#)]
- Marcos, P.M. Functionalization and Properties of Homooxalixarenes. In *Calixarenes and Beyond*; Neri, P., Sessler, J. L., Wang, M.-X., Eds.; Springer: Cham, Switzerland, 2016.
- Joseph, R.; Rao, C.P. Ion and Molecular Recognition by Lower Rim 1,3-Di-conjugates of Calix[4]arene as Receptors. *Chem. Rev.* **2011**, *111*, 4658–4702. [[CrossRef](#)] [[PubMed](#)]
- Wu, C.; Ikejiri, Y.; Zeng, X.; Elsegood, M.R.J.; Redshaw, C.; Yamato, T. Synthesis of Mono-*O*-alkylated Homooxalix[3]arene and a Protection–Deprotection Strategy for Homooxalix[3]arene. *Org. Lett.* **2017**, *19*, 66–69.
- Kumar, M.; Kumar, R.; Bhalla, V. Optical Chemosensor for Ag<sup>+</sup>, Fe<sup>3+</sup>, and Cysteine: Information Processing at Molecular Level. *Org. Lett.* **2011**, *13*, 366–369. [[CrossRef](#)] [[PubMed](#)]
- Jung, H.S.; Kwon, P.S.; Lee, J. W.; Kim, J.I.; Hong, C.S.; Kim, J.; Yan, W.S.; Lee, J.Y.; Lee, J.H.; Joo, T.; et al. Coumarin-derived Cu(2+)-selective fluorescence sensor: synthesis, mechanisms, and applications in living cells. *J. Am. Chem. Soc.* **2009**, *131*, 2008–2012. [[CrossRef](#)] [[PubMed](#)]
- Gutsche, C.D. Shaping the Baskets: Conformations of Calixarenes. In *Calixarenes. An Introduction*; Stoddart, J.F., Ed.; The Royal Society of Chemistry: Cambridge, UK, 2008.
- Cottet, K.; Marcos, P.M.; Cragg, P.J. Fifty years of oxalix[3]arenes: A review. *Beilstein J. Org. Chem.* **2012**, *8*, 201–226. [[CrossRef](#)] [[PubMed](#)]
- Ni, X.-L.; Takimoto, M.; Zeng, X.; Yamato, T. Synthesis, structure and inclusion properties of cone-tris{[(5'-methyl-2,2'-bipyridyl)-5-yl]oxycarbonylmethoxy}hexahomotrioxalix[3]arene. *J. Incl. Phenom. Macrocycl. Chem.* **2011**, *71*, 231–237. [[CrossRef](#)]
- Wu, C.; Ikejiri, Y.; Zhao, J.-L.; Jiang, X.-K.; Ni, X.-L.; Zeng, X.; Redshaw, C.; Yamato, T. A pyrene-functionalized triazole-linked hexahomotrioxalix[3]arene as a fluorescent chemosensor for Zn<sup>2+</sup> ions. *Sens. Actuators B* **2016**, *228*, 480–485. [[CrossRef](#)]
- Wu, C.; Wang, C.-Z.; Zhu, Q.; Zeng, X.; Redshaw, C.; Yamato, T. Click synthesis of a quinoline-functionalized hexahomotrioxalix[3]arene: A turn-on fluorescence chemosensor for Fe<sup>3+</sup>. *Sens. Actuators B* **2018**, *254*, 52–58. [[CrossRef](#)]
- Tsubaki, K.; Otsubo, T.; Morimoto, T.; Maruoka, H.; Furukawa, M.; Momose, Y.; Shang, M.H.; Fujii, K. Modification of the Upper Rim of Homooxalix[3]arenes and Complexation between a Nitrohomooxalix[3]arene Derivative and *n*-Hexylamine. *J. Org. Chem.* **2002**, *67*, 8151–8156. [[CrossRef](#)] [[PubMed](#)]
- Yamato, T.; Rahman, S.; Kitajima, F.; Zeng, X.; Gil, J.T. Synthesis and inclusion properties of *O*-tris(benzyloxy)hexahomotrioxalix[3]arenes. *J. Chem. Res.* **2006**, *8*, 496–498. [[CrossRef](#)]
- Ikeda, A.; Hatano, T.; Shinkai, S.; Akiyama, T.; Yamada, S. Efficient Photocurrent Generation in Novel Self-Assembled Multilayers Comprised of [60]Fullerene–Cationic Homooxalix[3]arene Inclusion Complex and Anionic Porphyrin Polymer. *J. Am. Chem. Soc.* **2001**, *123*, 4855–4856. [[CrossRef](#)] [[PubMed](#)]
- Ikeda, A.; Yoshimura, M.; Udzu, H.; Fukuhara, C.; Shinkai, S. Inclusion of [60]Fullerene in a Homooxalix[3]arene-Based Dimeric Capsule Cross-Linked by a Pd<sup>II</sup>–Pyridine Interaction. *J. Am. Chem. Soc.* **1999**, *121*, 4296–4297. [[CrossRef](#)]
- Schmidtchen, F.P.; Berger, M. Artificial Organic Host Molecules for Anions. *Chem. Rev.* **1997**, *97*, 1609. [[CrossRef](#)] [[PubMed](#)]

20. Beer, P.D.; Gale, P.A. Anion Recognition and Sensing: The State of the Art and Future Perspectives. *Angew. Chem. Int. Ed.* **2001**, *40*, 486–516. [[CrossRef](#)]
21. Sansone, F.; Baldini, L.; Casnati, A.; Ungaro, R. Calixarenes: from biomimetic receptors to multivalent ligands for biomolecular recognition. *New J. Chem.* **2010**, *34*, 2715–2728. [[CrossRef](#)]
22. Casnati, A.; Pochini, A.; Ungaro, R.; Ugozzoli, F.; Arnaud, F.; Fanni, S.; Schwing, M.-J.; Egberink, R.J.; de Jong, F.; Reinhoudt, D.N. Synthesis, Complexation, and Membrane Transport Studies of 1,3-Alternate Calix[4]arene-crown-6 Conformers: A New Class of Cesium Selective Ionophores. *J. Am. Chem. Soc.* **1995**, *117*, 2767–2777. [[CrossRef](#)]
23. Yamamoto, H.; Ueda, K.; Suenaga, H.; Sakaki, T.; Shinkai, S. Exploitation of Na<sup>+</sup>-Selective Electrodes for Protein Solutions from Crown-Bridged Calix[4]quinones. *Chem. Lett.* **1996**, *25*, 39–40. [[CrossRef](#)]
24. Dozol, J.F.; Ludwig, R. Extraction of Radioactive by Calixarenes. *Elements Ion Exch. Solvent Extr.* **2010**, *19*, 195–310.
25. Ludwig, R.; Dzung, N.T.K. Calixarene-Based Molecules for Cation Recognition. *Sensors* **2002**, *2*, 397–416. [[CrossRef](#)]
26. Ni, X.-L.; Wang, S.; Zeng, X.; Tao, Z.; Yamato, T. Pyrene-Linked Triazole-Modified Homooxalix[3]arene: A Unique C<sub>3</sub> Symmetry Ratiometric Fluorescent Chemosensor for Pb<sup>2+</sup>. *Org. Lett.* **2011**, *13*, 552–555. [[CrossRef](#)] [[PubMed](#)]
27. Ni, X.-L.; Zeng, X.; Redshaw, C.; Yamato, T. Synthesis and evaluation of a novel pyrenyl-appended triazole-based thiacalix[4]arene as a fluorescent sensor for Ag<sup>+</sup> ion. *Tetrahedron* **2011**, *67*, 3248–3253. [[CrossRef](#)]
28. Jiang, X.K.; Ikejiri, Y.; Jin, C.C.; Wu, C.; Zhao, J.L.; Ni, X.-L.; Zeng, X.; Redshaw, C.; Yamato, T. Synthesis and evaluation of a novel fluorescent sensor based on hexahomotrioxalix[3]arene for Zn<sup>2+</sup> and Cd<sup>2+</sup>. *Tetrahedron* **2016**, *72*, 4854–4858. [[CrossRef](#)]
29. Yamato, T.; Kitajima, F.; Gil, J.T. Alkyl Ammonium Ion Selectivity of Hexahomotrioxalix[3]arene Triamide Derivative having the Intramolecular Hydrogen-bonding Group. *J. Incl. Phenom. Macrocycl. Chem.* **2005**, *53*, 257–262. [[CrossRef](#)]
30. Yamato, T.; Zhang, F.; Tsuzuki, H.; Miura, Y. Synthesis and Inclusion Properties of C<sub>3</sub>-Symmetrically Capped Hexahomotrioxalix[3]arenes with Ester Groups on the Lower Rim. *Eur. J. Org. Chem.* **2001**, 1069–1075. [[CrossRef](#)]
31. Yamato, T.; Zhang, F. Synthesis, conformations and inclusion properties of hexahomotrioxalix[3]arene triamide derivatives having hydrogen-bonding groups. *J. Incl. Phenom. Macrocycl. Chem.* **2001**, *39*, 55–64. [[CrossRef](#)]
32. Takeshita, M.; Shinkai, S. Novel fluorometric sensing of ammonium ions by pyrene functionalized homotrioxalix[3]arenes. *Chem. Lett.* **1994**, *32*, 125–128. [[CrossRef](#)]
33. Gabba, F.P.; Schier, A.; Riede, J.; Hynes, M.J. Recognition of 1,2-diazines by a bidentate Lewis acid. *Chem. Commun.* **1998**, *8*, 897–898. [[CrossRef](#)]
34. Rostovtsev, V.V.; Green, L.G.; Fokin, V.V.; Sharpless, K.B. A Stepwise Huisgen Cycloaddition Process: Copper(I)-Catalyzed Regioselective “Ligation” of Azides and Terminal Alkynes. *Angew. Chem. Int. Ed.* **2002**, *41*, 2596–2599. [[CrossRef](#)]
35. Bifulco, G.; Riccio, R.; Gaeta, C.; Neri, P. Quantum Mechanical Calculations of Conformationally Relevant <sup>1</sup>H and <sup>13</sup>C-NMR Chemical Shifts of N-, O-, and S-Substituted Calixarene Systems. *Chem. Eur. J.* **2007**, *13*, 7185–7194. [[CrossRef](#)] [[PubMed](#)]
36. Araki, K.; Hashimoto, N.; Otsuka, H.; Shinkai, S. Synthesis and ion selectivity of conformers derived from hexahomotrioxalix[3]arene. *J. Org. Chem.* **1993**, *58*, 5958–5963. [[CrossRef](#)]
37. Raymo, F.M.; Stoddart, J.F. Interlocked Macromolecules. *Chem. Rev.* **1999**, *99*, 1643–1664. [[CrossRef](#)] [[PubMed](#)]
38. Cafeo, G.; Gargiulli, C.; Gattuso, G.; Kohnke, F.H.; Notti, A.; Occhipinti, S.; Pappalardo, S.; Parisi, M.F. Recognition and binding of paraquat dichloride by cyclodextrin/calix[6]pyrrole binary host systems. *Tetrahedron Lett.* **2002**, *43*, 8103–8106. [[CrossRef](#)]

39. Ikeda, A.; Udzu, H.; Zhong, Z.; Shinkai, S.; Sakamoto, S.; Yamaguchi, K. A Self-Assembled Homooxalix[3]arene-based Dimeric Capsule Constructed by a Pd<sup>II</sup>–Pyridine Interaction Which Shows a Novel Chiral Twisting Motion in Response to Guest Inclusion. *J. Am. Chem. Soc.* **2001**, *123*, 3872–3877. [[CrossRef](#)] [[PubMed](#)]
40. Prins, L.J.; Huskens, J.; de Jong, F.; Timmerman, P.; Reinhoudt, D.N. Complete asymmetric induction of supramolecular chirality in a hydrogen-bonded assembly. *Nature* **1999**, *398*, 498–502. [[CrossRef](#)]
41. Prins, L.J.; Jolliffe, K.A.; Hulst, R.; Timmerman, P.; Reinhoudt, D.N. Control of Structural Isomerism in Noncovalent Hydrogen-Bonded Assemblies Using Peripheral Chiral Information. *J. Am. Chem. Soc.* **2000**, *122*, 3617–3627. [[CrossRef](#)]
42. Takimoto, M.; Ni, X.-L.; Rahman, S.; Zeng, X.; Yamato, T. Heteroditopic receptors tris(2-pyridylamide) derivatives derived from hexahomotrioxalix[3]arene triacetic acid. *J. Incl. Phenom. Macrocycl. Chem.* **2011**, *70*, 69–80. [[CrossRef](#)]
43. Perdew, J.P.; Burke, K.; Ernzerhof, M. Generalized Gradient Approximation Made Simple. *Phys. Rev. Lett.* **1996**, *77*, 3865. [[CrossRef](#)] [[PubMed](#)]
44. Perdew, J.P.; Burke, K.; Ernzerhof, M. Generalized Gradient Approximation Made Simple. *Phys. Rev. Lett.* **1997**, *78*, 1396. [[CrossRef](#)]
45. Hay, P.J.; Wadt, W.R. Ab initio effective core potentials for molecular calculations. Potentials for the transition metal atoms Sc to Hg. *J. Chem. Phys.* **1985**, *82*, 270. [[CrossRef](#)]
46. Wadt, W.R.; Hay, P.J.; Ab initio effective core potentials for molecular calculations. Potentials for main group elements Na to Bi. *J. Chem. Phys.* **1985**, *82*, 284.
47. Hay, P.J.; Wadt, W.R. Ab initio effective core potentials for molecular calculations. Potentials for K to Au including the outermost core orbitals. *J. Chem. Phys.* **1985**, *82*, 299. [[CrossRef](#)]
48. *Spartan'10*, version 1.1.0; Wavefunction Inc.: Irvine, CA, USA.
49. Frisch, M.J.; Trucks, G.W.; Schlegel, H.B.; Scuseria, G.E.; Robb, M.A.; Cheeseman, J.R.; Scalmani, G.; Barone, V.; Mennucci, B.; Petersson, G.A.; et al. *Gaussian 09*; Revision A.02; Gaussian, Inc.: Wallingford, CT, USA, 2013.
50. *SAINT and APEX*, version 2; Software for CCD Diffractometers; Bruker AXS Inc.: Madison, WI, USA, 2012.
51. Sheldrick, G.M. Crystal structure refinement with *SHELXL*. *Acta Crystallogr.* **2015**, *C71*, 3–8.
52. Van der Sluis, P.; Spek, A.L. BYPASS: an effective method for the refinement of crystal structures containing disordered solvent regions. *Acta Crystallogr.* **1990**, *A46*, 194–201. [[CrossRef](#)]

**Sample Availability:** Samples of the compound are not available from the authors.



© 2018 by the authors. Licensee MDPI, Basel, Switzerland. This article is an open access article distributed under the terms and conditions of the Creative Commons Attribution (CC BY) license (<http://creativecommons.org/licenses/by/4.0/>).